



## Modeling thermal conductivity in $\text{UO}_2$ with $\text{BeO}$ additions as a function of microstructure

D.S. Li<sup>a,\*</sup>, H. Garmestani<sup>a</sup>, J. Schwartz<sup>b,c</sup>

<sup>a</sup> School of Materials Science and Engineering, Georgia Institute of Technology, 771 Ferst Dr. Atlanta, GA 30332-0245, USA

<sup>b</sup> Department of Mechanical Engineering, Florida A&M University-Florida State University College of Engineering, Tallahassee, FL 32310, USA

<sup>c</sup> National High Magnetic Field Laboratory, Florida State University, Tallahassee, FL 32310, USA

### ARTICLE INFO

#### Article history:

Received 21 July 2008

Accepted 11 March 2009

### ABSTRACT

New processing methods show promise for improved thermal conductivity in  $\text{UO}_2$  by the incorporation of a highly-conducting material. Such composites are likely to have anisotropic microstructures which bring new challenges to thermal conductivity simulation but also significant potential for improvement in the thermal performance. This paper presents simulation results for the thermal conductivity of  $\text{UO}_2/\text{BeO}$  composites using statistical continuum mechanics. The results successfully capture the microstructural heterogeneity and predict the corresponding anisotropic thermal properties. The application of statistical continuum mechanics to materials design makes it possible to design novel anisotropic fuel pellets with enhanced thermal conductivity in a preferred direction.

© 2009 Elsevier B.V. All rights reserved.

### 1. Introduction

Uranium dioxide ( $\text{UO}_2$ ) is the most widely used nuclear fuel for fission reactors and is expected to remain such in future reactors as well. One of the primary limitations for present  $\text{UO}_2$  systems, which may also limit the performance of future systems, is poor thermal conductivity [1]. While oxide fuels such as  $\text{UO}_2$  have a high melting point allowing high fuel centerline temperature, low thermal conductivity results in high fuel temperature, increases fission gas release during irradiation and stores energy in the fuel, decreasing safety margins in accident scenarios [2]. Low thermal conductivity also introduces a steep temperature gradient within  $\text{UO}_2$  pellets, resulting in large thermal stresses which in turn may initiate fuel restructuring, plastic deformation and cracking. Further complicating reactor design,  $\text{UO}_2$  thermal conductivity decreases significantly with increasing temperature [3–5], further decreasing the coolant outlet temperature for the same fission rate. Regardless of the specific nuclear fuel design, the fuel is subject to temperature gradients which affect heat removal and overall reactor performance. These thermal gradients strongly influence the thermo-mechanical, structural and chemical behavior of the fuel. Thus, while the impact of higher fuel thermal conductivity on overall reactor performance depends greatly on the details of the specific reactor design, increased thermal conductivity is desirable, particularly for future high-performance nuclear reactor systems.

Modeling the thermal conductivity of innovative nuclear fuel concepts with microstructures significantly different from

conventional  $\text{UO}_2$  is important for the development of next generation nuclear fuel materials. The temperature distribution within fuel pellets is vital to reactor performance, including effects on heat transfer, grain growth/restructuring, mechanical behavior, pellet/clad interactions, fission product migration and fission gas release. While several sophisticated techniques have been developed to predict the fuel thermal conductivity, most of the current models concentrate on the evolution of thermal conductivity with temperature. The influence of molecular structure, lattice parameter and conductive mechanism have been investigated thoroughly and several empirical and theoretical laws have been proposed [6–8]. The influence of microstructure, however, has not been addressed in the modeling of thermal conductivity because traditional fuel pellets exhibit random microstructures and thus possess isotropic properties. Such randomness, a hidden assumption in most current models, does not facilitate the prediction of thermal conductivity in fuels with engineered microstructures which can be designed with anisotropic properties that may ultimately be preferred.

Several approaches are under development to improve the thermal conductivity of  $\text{UO}_2$  fuel, including techniques that incorporate a highly conducting phase into the  $\text{UO}_2$ . For example, co-sintering has been used to form a continuous second phase of  $\text{BeO}$  to improve the thermal conductivity [9,10].  $\text{BeO}$  has high thermal conductivity and excellent chemical compatibility with  $\text{UO}_2$  and  $\text{UO}_2/\text{BeO}$  has been shown by a few groups to exhibit superior thermal performance [11,12]. Other  $\text{UO}_2$  composites include  $\text{UO}_2$  with  $\text{SiC}$  whiskers [9,10], with  $\text{W}$  continuous channels [13] or with  $\text{SnO}_2$  [14]. These composites all showed improved behavior with anisotropic microstructures which are significantly different from the traditional  $\text{UO}_2$  microstructure. In a cylindrical fuel pellets and

\* Corresponding author. Tel.: +1 4043854495; fax: +1 4048949140.  
E-mail address: [dli@gatech.edu](mailto:dli@gatech.edu) (D.S. Li).

rods, the thermal conductivity in the radial direction is significantly more important than that along the axial direction. Thus, designing fuel pellets with anisotropic thermal conductivity may be an attractive option for improved fuel and reactor performance.

Here, a statistical continuum mechanics approach is used to evaluate the impact of an anisotropic microstructure on the thermal conductivity of oxide composites. Homogenization relations based on statistical approaches are at the heart of the microstructure sensitive design (MSD) approach proposed to facilitate formulation of a highly efficient spectral linkage among microstructure distribution functions, macroscale effective properties and processing history. By linking microstructure, properties and processing, solutions to the inverse problems encountered in the customized design of composite materials for superior performance in targeted applications are found [15]. The success of the first-order MSD methodology has been demonstrated in several design applications and is reaching maturity [16–19]. The mathematical representation of microstructures through the probability density functions and their linkage to thermal properties are discussed in Sections 2 and 3. The approach is then applied in Section 4 to UO<sub>2</sub>/BeO composites, demonstrating the significant potential of both the MSD framework for oxide composite development and that of UO<sub>2</sub>/BeO composites with tailored microstructures for future nuclear fuels.

## 2. Correlation functions characterizing heterogeneous media

The microstructure of a heterogeneous medium can be described statistically and digitized by an  $n$ -point probability distribution function. Volume fraction, commonly used to capture the complexity of a microstructure, is a *de facto* one-point probability distribution function. Consider a composite with UO<sub>2</sub> as phase 1 and a highly conducting second phase such as a BeO coating or embedded nanoparticles (e.g., SiC or TiO<sub>2</sub>) as phase 2. Let the sample occupy a subset of space  $V \subset R^d (d = 3)$  that is partitioned into two disjoint phases: UO<sub>2</sub> in subspace  $V_1$  and BeO in subspace  $V_2$ . These subspaces satisfy:  $V = V_1 \cup V_2$  and  $V_1 \cap V_2 = \Phi$ . An indicator function  $L^i(x)$  for phase  $i$  is used to identify a random point  $x$ , located either inside or outside of phase  $i$ :

$$L^i(x) = \begin{cases} 1, & x \in V_i \\ 0, & \text{otherwise.} \end{cases} \quad (1)$$

By definition,  $\phi_i$ , the volume fraction for phase  $i$ , is a one-point correlation function

$$\phi_i = P\{L^i(x) = 1\}. \quad (2)$$

It is clear that volume fraction alone cannot capture the whole complexity of morphology in a random heterogeneous medium when studying effective properties. This may be demonstrated by the difference observed when two bounding theories, series and parallel, are used to predict the properties for a composite with equal constituent volume fractions. Specific details of the shape and morphology of the microstructure, including the interaction of the components and orientation distributions of polycrystals (texture), must be considered to obtain an accurate prediction of effective properties. This can only be realized using higher order distribution functions. A two-point distribution function is defined as a probability function when the statistics of a three-dimensional vector,  $\vec{r} = \vec{r}_2 - \vec{r}_1$ , is investigated once attached to each set of random points in a particular microstructure:

$$P_{i_1 i_2}(\vec{r}) = P_{i_1 i_2}(\vec{r}_2 - \vec{r}_1) = P\{L^{i_1}(\vec{r}_1) = 1, L^{i_2}(\vec{r}_2) = 1\}. \quad (3)$$

Here  $P_{i_1 i_2}(\vec{r}_2 - \vec{r}_1)$  is the probability of the event  $\vec{r}$  with vector  $\vec{r}_1$  in phase  $i_1$  and vector  $\vec{r}_2$  in phase  $i_2$ . It should be noted that, in many cases, the medium is anisotropic and it is inappropriate to simplify the vector to its magnitude, a scalar parameter.

The most common formula to represent the two-point correlation is an exponential function proposed by Corson [20].

$$P_{ij}(\vec{r}) = v_i v_j + (-1)^{i+j} v_i v_j \exp(-c_{ij} r^{n_{ij}}), \quad (4)$$

where  $P_{ij}(\vec{r})$  is the probability of a vector  $\vec{r}$  with head in phase  $i$  and tail in phase  $j$ .  $v_i$  and  $v_j$  are volume fractions of phase  $i$  and  $j$ , respectively. The constants  $c_{ij}$  and  $n_{ij}$  are microstructural parameters. For a two-phase composite (including porous materials),  $i$  and  $j$  correspond to phases 1 and 2; for multiphase materials, including composites,  $i$  and  $j$  vary from 1 to the total number of phases present. This relationship is appropriate only for random isotropic microstructures because the vector directions are not considered. Saheli et al. [15] introduced a simplified form for anisotropic two-point correlation:

$$P_{ij}(\vec{r}(r, \theta)) = v_i v_j + (-1)^{i+j} v_i v_j \exp(-c_{ij}(\theta) r). \quad (5)$$

The vector  $\vec{r}$  is not only the function of its own magnitude  $r$ , but also its direction,  $\theta$ , representing the angle between the vector and the horizontal direction. The formulation is applied to two-dimensional microstructures. The empirical coefficient  $c_{ij}$ , a scaling parameter representing the correlation distance, is reformulated by a Fourier expansion. If only the first order term is taken into account, then,

$$c_{ij}(\theta) = c_{ij}^0 (1 + (1 - A) \sin \theta), \quad (6)$$

where  $A$  is a material parameter that represents the degree of anisotropy in a microstructure such that  $A = 1$  corresponds to an isotropic microstructure, and  $c_{ij}^0$  is the reference empirical coefficient.

In this study, for an anisotropic heterogeneous sample, a three dimensional form of the correlation function is proposed:

$$P_{ij}(\vec{r}(r, \theta, \phi)) = v_i v_j + (-1)^{i+j} v_i v_j \exp(-c_{ij}(\theta, \phi) r). \quad (7)$$

The vector  $\vec{r}$  is a function of magnitude  $r$ , azimuthal angle  $\theta$ , and polar angle  $\phi$ . This formula is used to represent the microstructure of a heterogeneous medium.

## 3. Statistical continuum model for thermal conductivity

We assume that a heterogeneous medium is composed of  $n$  constituents with different conductivities,  $m^i$ , ( $i = 1 \dots n$ ) and partitions  $v^i$ . The local heat flux  $q$  and local temperature gradient  $-\nabla T$  at any arbitrary point  $x$  satisfy the linear relationship such that:

$$q(x) = -k(x) - T(x), \quad (8)$$

where  $k(x)$  is the local thermal conductivity. The effective thermal conductivity in the heterogeneous medium,  $k_{eff}$ , is then defined by:

$$\langle q(x) \rangle = -k_{eff} \langle \nabla T(x) \rangle, \quad (9)$$

where  $\langle \dots \rangle$  denotes the ensemble average. To obtain  $k_{eff}$ , one first defines the relationship between the localized conductivity  $k(x)$  and the ensemble average of the thermal conductivity,  $k_0$  by introducing the polarized conductivity  $\tilde{k}(x)$  such that:

$$k(x) = k_0 + \tilde{k}(x). \quad (10)$$

If we define the polarized field  $P(x)$  as:

$$P(x) = \tilde{k}(x) \nabla T(x), \quad (11)$$

then we have:

$$q(x) = -k_0 \nabla T(x) + P(x). \quad (12)$$

In calculating the thermal behavior of the system, we assume that there is no heat generated in the oxide composite. This is a significant simplification relative to the in-service behavior of nuclear fuel. As a result, this approach is appropriate for determining the

effective thermal conductivities of the composite materials, but it is not the mathematical representation that one would use to evaluate a fuel pellet or fuel rod design. With this simplification, the heat flux is divergence free:

$$\nabla \cdot q(x) = 0 = -k_0 \nabla \cdot \nabla T(x) + \nabla \cdot P(x), \quad (13)$$

which simplifies to:

$$k_0 \nabla \cdot (\nabla T) = \nabla \cdot P(x). \quad (14)$$

Eq. (14) can be solved using a number of techniques including a Green's function, which results in a solution:

$$T(x) = T_0(x) - \int dx' \nabla g(x, x') P(x'), \quad (15)$$

$$g(x, x') = \frac{1}{4\pi\sigma_0} \frac{1}{x - x'}, \quad (16)$$

where  $T_0$  is the reference temperature. To obtain the temperature gradient field, Eq. (15) is differentiated:

$$\nabla T(x) = \nabla T_0 + \int dx' G(x - x') * \tilde{k}(x') \nabla T(x'), \quad (17)$$

where  $\nabla T_0$  is the applied temperature gradient. The solution to the Green's function  $G(x - x')$  is derived elsewhere [21]; here we describe a numerical routine to perform the integration over the Green's function for an ensemble of aggregates in a heterogeneous medium. Because of the existence of a singular point in the integral at  $x = x'$ , a spherical region around the singular point must be excluded. Using integration by parts and the divergence theorem, the Green's function  $G(x - x')$  is expressed as:

$$G(x - x') = -D\delta(x - x') + H(x - x'), \quad (18)$$

$$\text{where } D = \frac{1}{3\sigma_0} I \text{ and } H = \frac{1}{4\pi\sigma_0} \frac{3\hat{n}\hat{n} - I}{r^3}, \quad (19)$$

where  $I$  is the second order identity tensor and  $\hat{n}$  is the unit vector of  $x - x'$ .

Substituting Eq. (11) into Eq. (17):

$$\nabla T(x) = \nabla T_0 + \int dx' G(x - x') * \tilde{k}(x') \nabla T(x'). \quad (20)$$

Using a Taylor series expansion and taking into account only the first-order correction results in:

$$\nabla T(x) = \nabla T_0 + \int dx' G(x - x') * \tilde{\sigma}(\nabla T_0, h(x')) \nabla T_0. \quad (21)$$

The average field for state  $h$  can be calculated from the above equation:

$$\langle \nabla T(x) \rangle_h = \nabla T_0 + \int dx' G(x - x') * \langle \tilde{k}(\nabla T_0, h(x')) \rangle_h \nabla T_0, \quad (22)$$

The correlation function  $\langle \tilde{k}(\nabla T_0, h(x')) \rangle_h$  can be described in terms of the conditional two-point probability density function of state  $h$ ,

$$\langle \tilde{k}(\nabla T_0, h(x')) \rangle_h = \int f(r' \in h(r') | r \in h) \tilde{k}(\nabla T_0, h(x')) dh(r'), \quad (23)$$

where the conditional two-point correlation function  $f(r' \in h(r') | r \in h)$  is defined as the probability of occurrence of  $r'$  at state  $h(r')$  given that  $r$  belongs to state  $h$ :

$$f(r' \in h_j | r \in h_i) = P_{ij}/V_i. \quad (24)$$

The corresponding two-point probability function  $P_{ij}(r, r')$  can be represented as:

$$P_{ij}(r, r') = v_i v_j + (-1)^{i+j} v_i v_j \exp(-c_{ij}(\theta, \phi) |r - r'|). \quad (25)$$

Since no assumption is used to represent the statistical distribution of constituents in the heterogeneous medium, the application of this statistical continuum model to the prediction of thermal conductivity covers a broad range of materials systems over a broad range of temperatures, assuming that the thermal conductivities of the individual constituents is known.

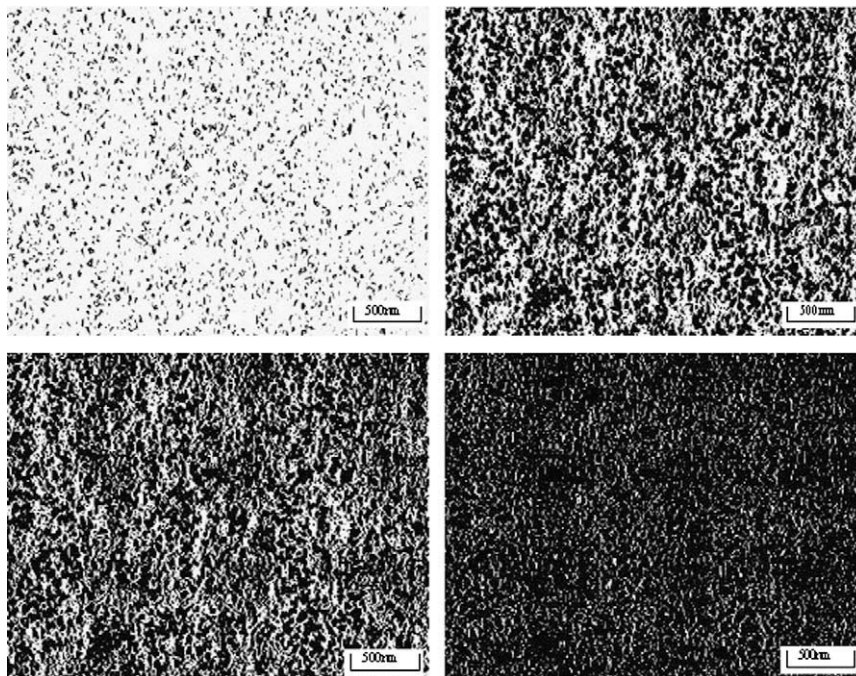


Fig. 1. Computer-generated simulated microstructures of relatively isotropic, heterogeneous composites of  $\text{UO}_2$  (white phase) with (a) 10%, (b) 40%, (c) 70% and (d) 90%  $\text{BeO}$  (black phase) inclusions.

#### 4. Simulation results and discussion

The formulation is applied to the prediction of the thermal conductivity of a  $\text{UO}_2/\text{BeO}$  composite. The room temperature thermal conductivity of  $\text{UO}_2$  is  $\sigma_1 = k_{\text{UO}_2} = 3.5 \text{ W}/(\text{m} \cdot \text{K})$  [1,3,4] and the room temperature thermal conductivity of  $\text{BeO}$  is  $\sigma_2 = k_{\text{BeO}} = 300 \text{ W}/(\text{m} \cdot \text{K})$  [22]. These values are relatively temperature independent over the range of interest.

To apply the statistical continuum mechanics formulation to the evaluation of heterogeneous composite thermal properties, it is necessary to hypothesize not only the relative volume fractions of the constituent phases (in this case  $\text{UO}_2$  and  $\text{BeO}$ ) but also some specifics regarding the microstructure. For this work, representative microstructures were developed such that both the relative volume fractions of  $\text{UO}_2$  and  $\text{BeO}$  are varied but also the degree of anisotropy in the microstructure. Some of these microstructures are illustrated in Figs. 1 and 2. These two series of microstructures are simulated from two gray scale micrographs from two samples with different anisotropy. Microstructures in Fig. 1 are from a relatively isotropic sample while those in Fig. 2 are from a more anisotropic sample. By adjusting the threshold during image segmentation, binary images representing different volume fractions of the second phase were generated. In this way, the simulated microstructures will maintain similar anisotropy and configuration despite varying the relative volume fractions of each phase. Thus, the microstructures illustrated in Fig. 1(a)–(d) are nearly isotropic examples for which only the  $\text{BeO}$  volume fraction varies, while those in Fig. 2(a)–(d), which have similar  $\text{BeO}$  volume fractions as in Fig. 1, are clearly anisotropic. Fig. 3 illustrates the thermal conductivities predicted by statistical continuum model for the series of isotropic microstructures shown in Fig. 1. Also shown are upper-bound and lower-bound curves, where the upper-bound curve is calculated using Taylor's model [23] based upon an orthotropic composite with the heat flowing parallel to both phases and

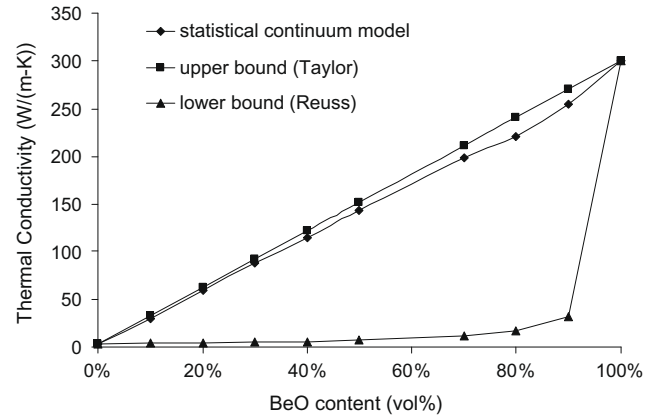


Fig. 3. Simulated thermal conductivity along the  $x$  direction of  $\text{UO}_2/\text{BeO}$  composites with microstructures illustrated in Fig. 1. The upper-bound and lower-bound curves are results from a Taylor model and a Reuss' model, respectively.

the lower-bound is from Reuss' model [24] based upon the same composite geometry but the heat flowing orthogonal (i.e., through each phase in-series). According to the homogenization relation, and depending on the specific microstructure design, an order-of-magnitude increase in thermal conductivity, from 3.5 to 30  $\text{W}/(\text{m} \cdot \text{K})$ , is obtained with a 10 vol.%  $\text{BeO}$  addition, and in general, the statistical continuum model shows that the thermal behavior of an isotropic composites with a well-dispersed conducting phase (such as those illustrated in Fig. 1) approaches that of the idealized upper-bound values.

The influence of microstructure, and in particular anisotropy, on the composite thermal conductivity is investigated by varying the degree of anisotropy for constant  $\text{BeO}$  content. The aim is to determine the possibility of increasing the thermal conductivity in one

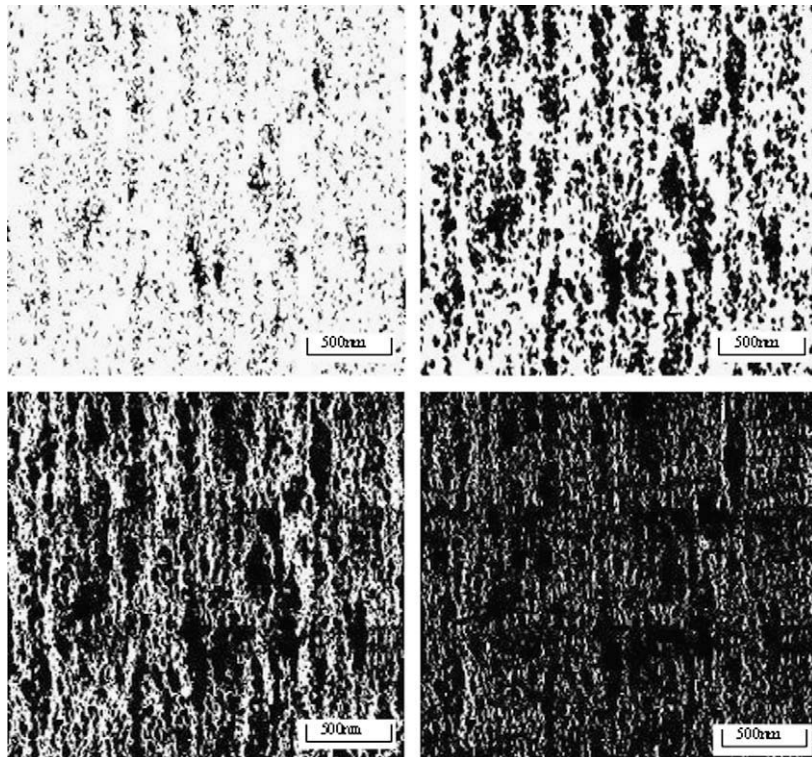


Fig. 2. Computer-generated simulated microstructures of anisotropic, heterogeneous composites of  $\text{UO}_2$  (white phase) with (a) 10%, (b) 40%, (c) 70% and (d) 90%  $\text{BeO}$  (black phase) inclusions.

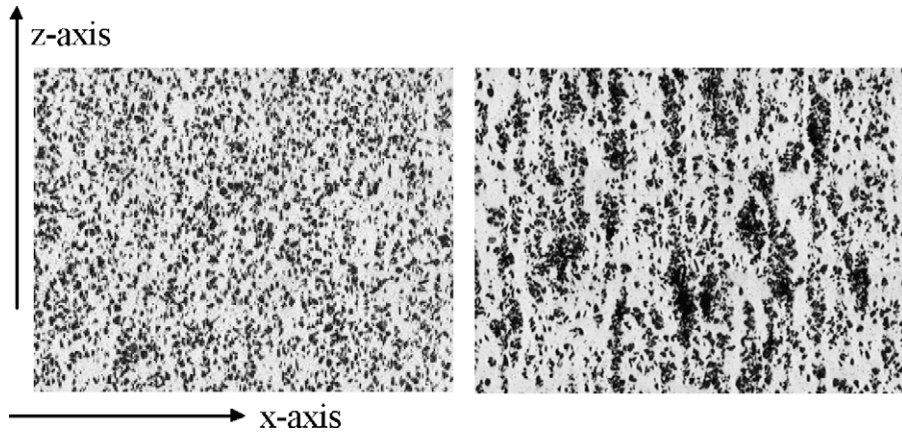


Fig. 4. Simulated micrographs of two UO<sub>2</sub>/BeO composites with 30% BeO. The white area is UO<sub>2</sub> and the black area is BeO. Both microstructures are anisotropic, with microstructure (a) less so than microstructure (b).

direction at the expense of another. In the case of a UO<sub>2</sub>/BeO composite for a fuel pellet, the aim would be to significantly improve the radial thermal conductivity through microstructural design. Fig. 4(a) and (b) show simulated microstructures of two UO<sub>2</sub>/BeO composites with a 30% BeO volume fraction but with different degrees of texturing (the microstructure shown in Fig. 4(a) being less anisotropic than that in Fig. 4(b)). The calculated thermal conductivities for these two microstructures, along with the values for the isotropic case shown in Fig. 1(b), are shown in Table 1.

Table 1  
Thermal conductivities of UO<sub>2</sub>/30% BeO composites with varying microstructures.

Microstructure	$k_x$ (W/m · K)	$k_z$ (W/m · K)	$k_z/k_x$
Isotropic	89.5	89.5	1.00
Less anisotropic	87.5	91.2	1.04
More anisotropic	86.5	91.7	1.06

The results in Table 1 illustrate that the statistical continuum mechanics formulation captures the microstructural anisotropy and predicts the anisotropic thermal conductivities. In sample a, with microstructure shown in Fig. 4(a), the thermal conductivity along z direction is 4.2% greater than that along x direction; while in sample b, with microstructure shown in Fig. 4(b), the thermal conductivity in the z direction is 6.1% greater than that in the x direction. Thus, there is a ~50% increase in the anisotropy of the thermal conductivity due to the microstructural change. Microstructural anisotropy can directly improve thermal conductivity in a preferred direction (at the expense of an orthogonal direction) if the desired microstructure can be obtained through processing.

This model can be extended to the MSD framework by bridging processing, microstructure and properties (e.g., thermal conductivity). A simplified processing path of this nature is illustrated in Fig. 5. The left panel of Fig. 5 is property closure, illustrating the range of properties the material system may possess. It is important to note that it is not limited to two dimensions or two types of properties. The properties used for optimization can be selected based

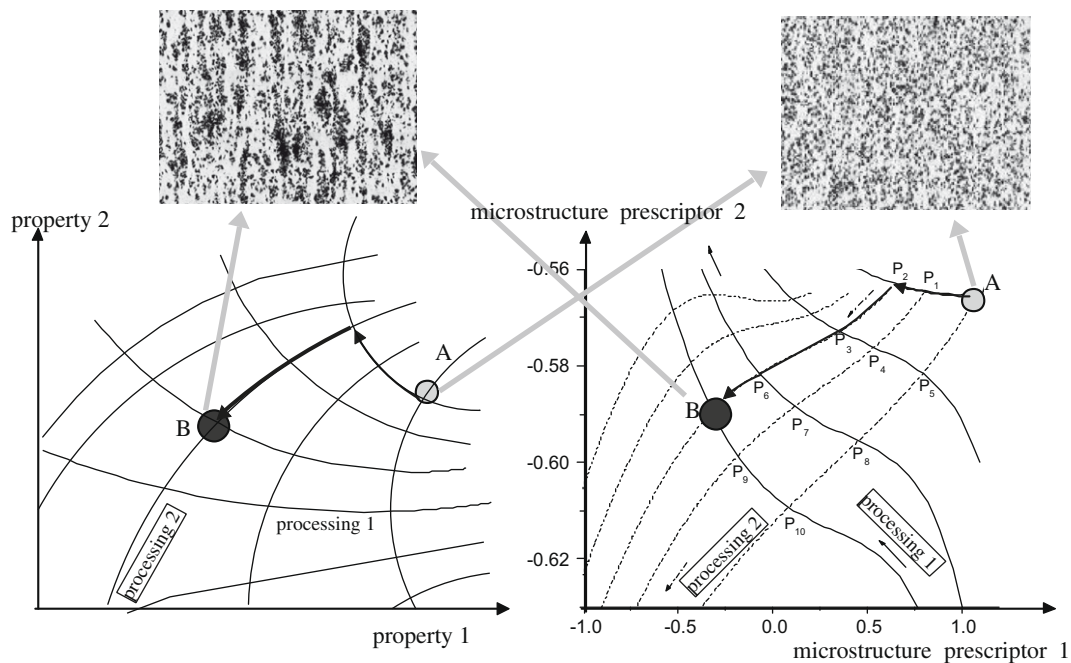


Fig. 5. Linkage between property closure and microstructure space in microstructure sensitive design, showing processing path to achieve desired microstructure by optimizing processing.

upon the material and application. In the example of nuclear fuel, it may include nuclear performance, thermal conductivity, thermal expansion, mechanical behavior, irradiation resistance, etc. The right panel of Fig. 5 is microstructure space in which the microstructure descriptors quantitatively describe the microstructure; each point represents an individual microstructure. Solid and dash lines in microstructure space illustrate how the microstructures evolve during processing. The corresponding lines in property closure illustrate how to achieve the desired properties with the target microstructure. To fully utilize the materials design approach to achieve the desired properties, an experimental database and corresponding modeling of the microstructural evolution during processing is required. Property prediction from the microstructure using statistical continuum models thus can facilitate fuel design with directionally-optimized thermal, mechanical, and nuclear performance.

## 5. Conclusions

The thermal conductivity of an anisotropic heterogeneous  $\text{UO}_2/\text{BeO}$  composite is predicted using a statistical continuum mechanics formulation that relies on a modified two-point correlation function to characterize the anisotropic microstructures. The results clearly show that the addition of BeO, which has very high thermal conductivity, within  $\text{UO}_2$  matrix, can greatly enhance the thermal performance of nuclear fuel in a preferred direction if

anisotropy can be engineered into the microstructure through processing. Such improvements will help the development of future, higher performance, nuclear reactor systems.

## References

- [1] C. Ronchi, *J. Phys.: Condens. Mat.* 6 (1994) L561.
- [2] M. Gavrilas et al., in: *Safety Features of Operating Light Water Reactors of Western*, CRC Press, 1995.
- [3] C. Ronchi et al., *J. Appl. Phys.* 85 (1999) 776.
- [4] C.G.S. Pillai, A.M. George, *J. Nucl. Mater.* 200 (1993) 78.
- [5] J.K. Fink, *J. Nucl. Mater.* 279 (2000) 1.
- [6] C. Ronchi, *High Temp.* 45 (2007) 552.
- [7] C.B. Basak, A.K. Sengupta, H.S. Kamath, *J. Alloy. Compd.* 360 (2003) 210.
- [8] J.K. Fink, *J. Nucl. Mater.* 279 (2000) 1.
- [9] K.H. Sarma et al., *J. Nucl. Mater.* 352 (2006) 324.
- [10] R. Latta, S.T. Revankar, A.A. Solomon, *Heat Transfer Eng.* 29 (2008) 357.
- [11] K. McCoy, C. Mays, *J. Nucl. Mater.* 375 (2008) 157.
- [12] S. Ishimoto et al., *J. Nucl. Sci. Technol.* 33 (1996) 134.
- [13] J.H. Yang et al., *J. Nucl. Mater.* 353 (2006) 202.
- [14] I.S. Kurina, V.V. Popov, V.N. Romyantsev, *Atom. Energ.* 101 (2006) 802.
- [15] G. Saheli, H. Garmestani, B.L. Adams, *J. Comput.-Aid. Des.* 11 (2005) 103.
- [16] B.L. Adams et al., *J. Mech. Phys. Solids* 49 (2001) 1639.
- [17] H. Garmestani et al., *Compos.: Part B* 31 (2000) 39.
- [18] H. Garmestani et al., *J. Mech. Phys. Solids* 49 (2001) 589.
- [19] S. Lin, H. Garmestani, B.L. Adams, *Int. J. Solids Struct.* 37 (2000) 423.
- [20] P.B. Corson, *J. Appl. Phys.* 45 (1974) 3159.
- [21] S. Torquato, *Heterogeneous Materials: Microstructure and Macroscopic Properties*, Springer-Verlag, New York, 2002.
- [22] G.A. Slack, S.B. Austerman, *J. Appl. Phys.* 42 (1971) 4713.
- [23] G.I. Taylor, *J. Inst. Met.* 62 (1938) 307.
- [24] A. Reuss, *Zeitschrift Fur Angewandte Mathematik Und Mechanik* 9 (1929) 49.